EXPERIMENTAL DYNAMIC PROPERTIES OF ABS CELLULAR BEAMS PRODUCED USING ADDITIVE MANUFACTURING

Apostolos Grammatikopoulos[1] , Joseph Banks[2] and Pandeli Temarel[3]

Fluid-Structure Interactions Group, University of Southampton
[1]Email: ag3e15@soton.ac.uk
[2]Email: J.Banks@soton.ac.uk
[3]Email: P.Temarel@soton.ac.uk

Keywords: additive manufacturing, cellular, flexural modulus, structural vibration, thin-walled girders

Abstract
Additive manufacturing is used increasingly for functional products and, consequently, the mechanical characterisation of the produced component has become a highly investigated topic. However, experimental routines consist mainly of tensile tests with standardised specimens and investigations focus on how process and design parameters, for example infill pattern, infill ratio, layering direction, affect the tensile modulus, ultimate elongation and strength.

In many cases, 3D printed components are subjected to static and/or dynamic bending operational loads and the flexural modulus should be identified. In polymers this can be significantly different, with an expected value between tensile and compressive moduli. Additionally, if the loading on the structure is dynamic (steady state or transient), dynamic (or vibratory) properties of the 3D printed structure become important. The present investigation focuses on methods for the experimental measurement of the flexural modulus under quasi-static and, more importantly, dynamic excitation. A range of structural approximations/numerical models are compared to identify the most suitable in providing the flexural modulus in a consistent manner.

1. Introduction

With additive manufacturing moving from being used solely for prototyping to production of experimental components and even end products, prediction of the mechanical properties becomes increasingly important. ABS and PLA are currently the most popular materials used for 3D printing, amongst others, due to ease of application and the industry's accumulated experience with such materials. Consequently, experimental research regarding 3D printed components revolves mainly around these two materials and, in some cases, the rapidly-emerging polycarbonates, the latter for enhanced mechanical properties and components subjected to higher loads.

Experimental investigations on the effect of design parameters on the mechanical properties of finished components have been quite extensive. Ahn et al [1] investigated the different infill patterns for ABS prints, as well as the relevant angles, and found significant effects on the tensile and compressive strengths of specimens. Rodríguez et al. [2] demonstrated the influence of the print meso-structure and infill ratio on the stress-strain response and particularly on the tensile modulus and strength. The results were compared to measurements from tensile testing of ABS filament and indicated reduction of mechanical properties through the filament deposition method. The measurements were then used to identify the printing parameters which optimize the mechanical behaviour of ABS components.

Es-Said et al. suggested that components produced with filament deposition resemble laminated materials in their orthotropic behaviour [3]. They also investigated how different layering directions affect yield strength and ultimate strength in tension, ultimate strength in bending and absorbed energy in impact. Although bending tests were performed in this case, no data was presented regarding the flexural modulus of the ABS specimens. Lee et al. [4], on the other hand, carried out experiments on the compressive strength of printed ABS components and demonstrated the anisotropic behaviour by applying loading in various directions. In this rare example of an investigation on the compressive properties of printed components, details regarding the compressive modulus were not provided.

As may be observed from the above, the focus of investigations is mainly set on failure modes and operational limits of the produced components. This can be explained by the fact that some applications only require the component to be sufficiently stiff and reliable and the precise value of the Young's modulus is not necessarily required. However, in the cases where a prediction of operational deflections and/or strains is critical, information in the literature only pertains to the tensile modulus. In the case of polymers, this can be quite different from the compressive modulus; in turn, the flexural modulus has a value between these two. It is recommended that, depending on the main loading direction (tensile/compressive/bending) on the structure under design, the relevant tests (tensile/compressive/flexural) are performed to calculate the appropriate modulus [5]. Moreover, due to the viscoelastic nature of polymers, the dynamic modulus in flexure can be different from the one observed under static or quasi-static loading.

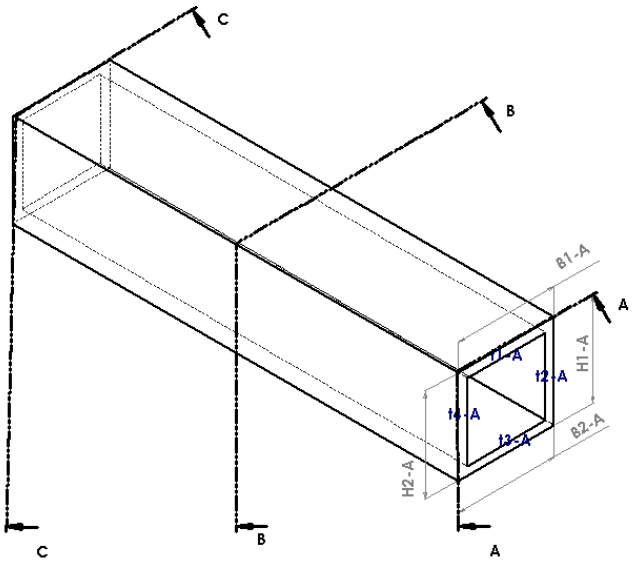

Figure 1: Depiction of the measurement points for each specimen segment. A, B and C denote the 3 sections where measurements were obtained. H, B and t represent measurements of height, breadth and thickness, respectively. No thickness measurements were obtained at the midpoint.

Our research is aimed at generating detailed elastic scaled models of ships, which requires prediction of the flexural modulus, to engineering accuracy standards, as it affects the natural frequency of the scaled ship model. The present investigation focuses on the vibratory responses of 3D printed hollow rectangular beams (see Figure 1) and the dynamic flexural modulus that is derived from them. Such components are part of the cellular arrangement of a container ship. To this end, a range of hollow rectangular uniform beams with various length/height ratios are tested using the modal testing (also known as impulse/impact excitation method [6]) and 3-point bending methods. Additional tests are carried out to examine the influence of transverse bulkheads in the middle and at the ends of the beam. The results are correlated using both Euler-Bernoulli and Timoshenko beam approximations and their

suitability is assessed by comparing against a shell structural model.

2. Methodology

2.1. Specimen production

Table 1: Specimen cross section details, with mean and standard deviation calculated for the entire population of specimens, rather than each specimen type separately (see Table 2).

Dimension	Symbol	Mean	SD
Breadth (m)	B	0.0280	9.88E-05
Height (m)	H	0.0273	7.62E-05
Thickness (m)	t	2.67E-03	6.31E-05
Cross-sectional Area (m^2)	A	2.68E-04	1.40E-06
2^{nd} Moment of Area (m^4)	I_{yy}	2.76E-08	1.52E-10
Mass/ Unit Length (kg/m)	μ	0.2622	0.0067

Table 2: Specimen type details, measured 2-node bending natural frequency (dynamic tests) and measured difference in load values corresponding to strains of 0.0025 and 0.0005 (3-point bending tests).

Specimen Type	L (m)		Number of Segments	Number of Specimens	Test Points	f_{2-node} (Hz)		$\Delta F_{\varepsilon=0.0005,0.0025}$ (N)	
	Mean	SD				Mean	SD	Mean	SD
A*	0.180		1	5	3	1372.47	22.43	124.82	6.75
B	0.180	1.21E-04	2	5	3	1381.53	9.52	93.51	17.67
C	0.256	1.00E-04	2	6	5	737.17	7.72	99.90	21.71
D†	0.260	9.77E-05	2	5	5	678.60	3.33	109.65	5.58
E	0.390	4.41E-04	3	5	8	340.46	2.93		
F	0.520	1.45E-04	4	3	11	194.33	0.90		

* Only nominal length available
† Including transverse bulkheads

For the purposes of this investigation, specimens of a constant, hollow rectangular cross section were manufactured using 3D printing. ABS was printed with an infill ratio of 99%, resulting in almost entirely solid structure. The layering direction was the same for all specimens and parallel to their longitudinal axis and the layer height used was 0.25 mm. Specimens of four different lengths were manufactured, namely 180 mm, 260 mm, 390 mm and 520 mm, in order to investigate the influence of beam-like behaviour. Details regarding the cross section may be found in Table 1.

In the case of 180 mm specimens, both a continuous version (A) and a version of two equal segments joined in the middle (B) were produced. The remaining specimens were all produced in segments of 130 mm. In all cases, the segments were joined together using a solution of the printing material (ABS) in acetone. The segments were constrained together using sash clamps while the acetone was evaporating to leave just ABS in the area of connection. An alternative version of the 260 mm specimens was produced, which included bulkheads at the ends and the middle of the specimen. A summary of all specimen types may be found in Table 2.

Extensive measurements were taken on each specimen segment prior to joining. Four thickness measurements, two breadth measurements and two height measurements were taken on each end of the segment. Two additional breadth and height measurements were taken at the midpoint of each segment. The measurement points are depicted in Figure 1. The measurements were used to calculate the cross-sectional

area and second moment of area at different points of each specimen (Table 1).

2.2. Experiments

The specimens were subjected to modal testing with both ends treated as free supports. They were tethered using flexible bands at the nodal locations of the 2-node bending mode, to minimise the influence of support on the aforementioned mode [7], which was the main focus of the investigation. The roving hammer setup used a PCB-086E80 instrumented hammer (sensitivity: ($\pm$20%) 22.5 mV/N) for the excitation measurement and a PCB-352C22 accelerometer (sensitivity: ($\pm$15%) 1.014 mV/m/s^2, frequency range: ($\pm$5%) 1.0 to 10000 Hz), located at one of the free ends of the specimen, for the response measurement. Both measurements were obtained using a DataPhysics Quattro Dynamic Signal Analyzer and SignalCalc software and the latter was also used for the calculation of the relevant frequency response functions.

5 specimens were tested for most specimen types (with two exceptions) and the number of measurement points increased with the length of the specimen. Details about numbers of specimens and measurement points,which were approximately evenly distributed along the length, may be found in Table 2. For each measurement point, the test was repeated thrice, the frequency response function was calculated for each repetition and an average was produced. The measured frequency range was between 0 and 2000 Hz (at a 0.5 Hz step), thus including the 2-node bending natural frequency for all lengths (see Table 2), and higher-order natural frequencies for the longer specimens.

The shorter specimen types (A, B, C, D) were also subjected to 3-point bending tests. A servo-mechanical INSTRON testing machine was used for this purpose. Specimen types E and F were not subjected to this type of testing due to maximum length restrictions. The specimens were supported by two circular rollers at 10% of the length from either end, emulating pinned-pinned boundary conditions. Both rollers had a diameter of 10 mm. A third roller of the same size applied a displacement at the midpoint of the specimen, descending at a speed of 2 mm/min. All the above parameters were based on the standard for the determination of flexural properties of plastics [8].

Both the experimental procedure and the post-processing method described above follow the relevant ASTM standard [6], with an increased number of measurement points. For static tests, this method was substituted by the procedure described in the relevant ISO Standard [8]. In this procedure, an Euler-Bernoulli beam approximation is assumed to calculate the modulus using the measurement points corresponding to strains of 0.0005 and 0.0025. In both types of tests, minor adjustments were made in the post-processing of results to account for differences in the specimen geometry compared to what is prescribed, as seen in the above equations.

2.3. Mathematical modelling

The specimen structure was then modelled using a number of different methods to investigate their validity for each specimen type. All values, including geometrical aspects, mass and experimental measurements (natural frequency, quasi-static extension & load) were averaged per specimen type for the purposes of these calculations.

As all the specimens, with the exception of specimen type D which included bulkheads, featured a uniform cross section and uniform mass distribution, the dynamic flexural modulus may be calculated with an Euler beam approximation, namely:

$$\omega_{2-node} = \frac{4.73^2}{L^2}\sqrt{\frac{EI}{\mu}} \tag{1}$$

where L is the specimen length, E the flexural modulus, I the 2^2 moment of area and μ the mass per unit length.

The second modelling method used a Timoshenko beam approach (element BEAM188 in ANSYS), whereas the third method employed a fully 3D FEA approach with shell elements including both membrane and bending loads (element SHELL181 in ANSYS). In all cases, an iterative process was followed to identify the flexural modulus E that resulted in the natural frequencies measured during the experiments. In all cases, lines were meshed with a maximum element length of 0.0009 m; that is to say, an element size of 0.0009 was used along all axes. The eigenvalue problem of the specimen with free-free boundary conditions was solved to compare to dynamic tests. The specimens were also modelled with roller support and a single applied deflection and the results were compared to the 3-point bending tests.

The range of different specimen types, combined with the aforementioned modelling techniques, was selected to allow a thorough understanding of their dynamic behaviour through the following process:

- establish (by comparing to shell modelling predictions) whether the vibrating specimens may be modelled using a beam approximation to derive the dynamic flexural modulus of the material from the 2-node bending natural frequency
- assess the suitability of the Euler beam method (as opposed to Timoshenko beam theory) depending on the length of the specimens and the importance of shear effects when calculating the aforementioned frequency
- investigate whether the inclusion of transverse bulkheads alters, in any way, the accuracy of these approximations.
- compare the produced values for the flexural modulus, from measured responses in quasi-static and dynamic conditions.

3. Results

3.1. Modal tests

The average 2-node vertical bending natural frequencies for the various specimen types are given in Table 2. Differences in natural frequencies between specimen types A and B (which have the same length and cross section) may be attributed to a larger thickness average on type A specimen, as well as the joining process for specimen type B. The more significant difference between specimen types C and D is due to the presence of transverse bulkheads in the latter which, although they don't affect the longitudinal stiffness, act as point masses at the local extrema of the 2-node bending mode shape (free ends and midpoint).

A summary of the dynamic flexural modulus estimations are shown in Figure 2. It may be observed that the shell element model provides us with with a consistent estimation of the dynamic flexural modulus (2.155 MPa with a standard deviation of 0.8%) over all specimen types. As this model includes both shear deformation effects in bending and section warping, it is considered the most general model and is used a baseline.

Estimations using the Timoshenko beam model are fairly close to the shell estimations (maximum difference of 3.5%) for most specimens, with the difference between the two increasing as specimens become shorter. This difference is attributed to warping of the cross section. Warping becomes less apparent in

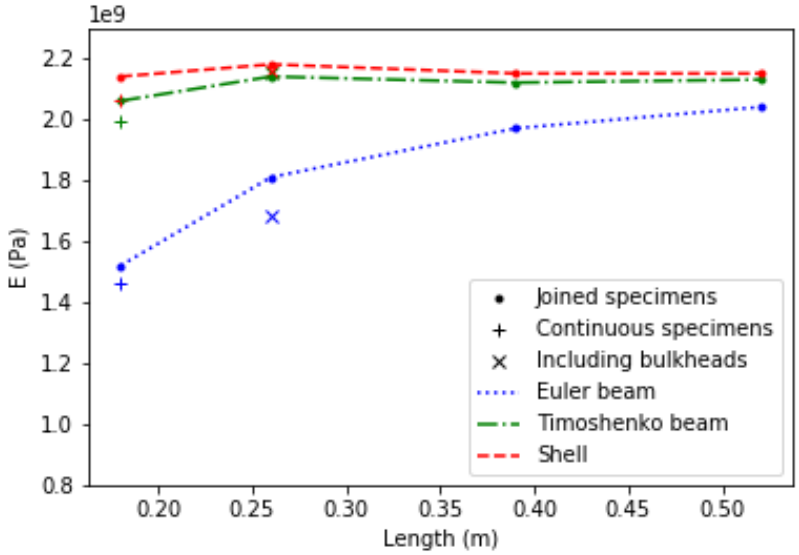

Figure 2: Dynamic flexural modulus of the specimens, derived from the 2-node bending natural frequency using three different structural models, as a function of specimen length. Lines (dot markers) depict specimens with no bulkheads, produced by joining a number of segments (see Table 2). + markers depict specimens without any joining, whereas x markers depict specimens including bulkheads.

longer specimens and from type C onwards the dynamic flexural modulus may be calculated using the Timoshenko beam approximation with difference from shell modelling of only 0.9%.

Estimations based on the Euler-Bernoulli beam approximation diverge much more significantly for shorter specimens. For the more slender specimens with a length of 520 mm the difference in calculated modulus from the shell element estimation is of the order of 5%. However, the difference rapidly increases with decreasing length, reaching 40% for the 180 mm specimens. It is evident that, for this scale of specimens, the 2-node bending natural frequency is significantly affected by shear deformation effects.Use of the Euler-Bernoulli beam approximation would only be recommended for the 520 mm specimens. This corresponds to a length/height ratio of 19, which is close to the ratio of 20 recommended by the standards (for beams with a rectangular rather than box-shaped cross section) [6, 8] to use the Euler beam approximation.

The continuous specimens (i.e. specimen type A) showed similar trends to the joined beams regarding the accuracy of the various approximations. When compared to specimen type B, comprising two segments, a slight increase in stiffness is observed caused by joining. The presence of bulkheads in specimen type D have two distinct effects. Firstly, the difference of the Euler beam results when compared to specimen type C signifies the importance of the mass distribution when calculating the natural frequency of these structures. Secondly, being the only specimen type where the Timoshenko beam and shell models coincide, it is emphasised that bulkheads prevent any deflection of the cross section and result in a structure that can be described just as well using a beam approximation.

3.2. 3-point bending tests

Results from the 3-point bending tests are shown in Figure 3. It can be observed that the trends for these quasi-static tests resembles the one previously discussed for the dynamic tests. The shell model suggests more consistent results for all specimen types tested, with the Timoshenko beam approximation slightly closer to these values for longer specimens and the Euler beam approximation having significantly larger

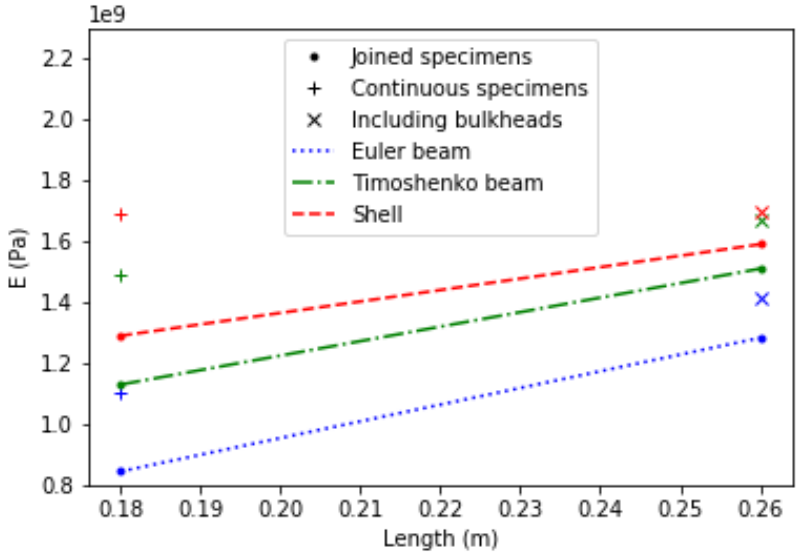

Figure 3: Quasi-static flexural modulus of the specimens, derived from the load-displacement curves using three different structural models, as a function of specimen length. Lines (dot markers) depict specimens with no bulkheads, produced by joining a number of segments (see Table 2). + markers depict specimens without any joining, whereas x markers depict specimens including bulkheads.

differences. It is also demonstrated that the quasi-static flexural modulus is approximately 35% lower than its dynamic counterpart. It may be concluded that identification of the quasi-static modulus would not be sufficient for the modelling of 3D printed structures which are subjected to dynamic loads.

The presence of bulkheads was found once more to restrict warping of the cross section and result in a specimen behaving more in a beam-like manner. As can be seen in Figure 3 the Timoshenko beam and shell approximations produced almost identical results (x-shaped markers). On the other hand, continuous specimens were found to produce responses indicating higher stiffness than the joined ones, contrary to what was found in vibration tests. Differences between the measured static and dynamic elastic modulus may be partly attributed to the viscoelastic nature of ABS. Furthermore, the experimental uncertainties associated with quasi-static and dynamic tests can be quite different, as illustrated by the mean and standard deviation values in Table 2, due to both the way the measurements are obtained and the nature of the physical problem investigated (load-deflection relationship or structural eigenvalue problem).

4. Conclusions

The present investigation examined the vibratory responses of 3D printed specimens with a thin-walled rectangular cross section. The main focus was the relationship between the 2-node bending natural frequency and the flexural modulus. The effects of joining specimens from segments and the effects of the presence of transverse bulkheads were also investigated. The specimens were subjected to modal testing, suspended using flexible bands at the 2-node bending nodes to emulate a free-free boundary condition. A range of different mathematical approximations were used to describe the dynamic behaviour and a dynamic flexural modulus was calculated based on the average measured 2-node bending natural frequency for each specimen type.

The shell element formulation was found to give consistent results for all specimen types and was used as a baseline. The Timoshenko beam approximation resulted in a flexural modulus estimation which

was very close to that of the shell approximation. A subtle increase in the difference between the two was observed for the very short specimens and was attributed to warping of the cross section. The Euler-Bernoulli beam approximation was found to produce more significant differences for this type of geometry, resulting in a difference from the shell model of the order of 5% for long specimens but increasing rapidly to 40% for the shortest specimens. Continuous specimens indicated that joining causes relatively small difference in the dynamic stiffness, whereas the presence of bulkheads resulted in a more beam-like behaviour.

Quasi-static 3-point bending tests demonstrated similar trends, whereas the quasi-static flexural modulus was found to be approximately 35% lower than the dynamic flexural modulus when using a shell approximation. The effects of joining on quasi-static responses appear to contradict the behaviour observed during dynamic tests, which may be attributed to the difference in nature between the two tests, resulting in different types of uncertainty. As observations on the continuous specimens and the ones including bulkheads were only based on one type of specimen, they should serve more as indicators and further investigation on these effects would be recommended.

Overall, dynamic tests and use of a Timoshenko beam approximation is recommended for the prediction of the dynamic properties of structures produced using additive manufacturing and materials similar to ABS. An elastic ship model with a cellular cross section resembling that of a container ship has been subjected to dynamic tests and it was established that 3-point bending tests are not appropriate for the prediction of its vibratory properties [9]. The flexural modulus of this model, obtained from the dynamic tests, was found to agree well with the Timoshenko beam and shell predictions in Figure 2.

Acknowledgements

The present investigation was funded by the Lloyd's Register Foundation University Technology Center on Ship Design for Enhanced Environmental Performance.

References

[1] S.-H. Ahn, M. Montero, D. Odell, S. Roundy, and P. K. Wright, "Anisotropic material properties of fused deposition modeling ABS," *Rapid Prototyping Journal*, vol. 8, no. 4, pp. 248–257, 2002.

[2] J. F. Rodríguez, J. P. Thomas, and J. E. Renaud, "Mechanical behavior of acrylonitrile butadiene styrene (ABS) fused deposition materials modeling," *Rapid Prototyping Journal*, vol. 9, no. 4, pp. 219–230, 2003.

[3] O. S. Es-Said, J. Foyos, R. Noorani, M. Mendelson, R. Marloth, and B. A. Pregger, "Effect of Layer Orientation on Mechanical Properties of Rapid Prototyped Samples," *Materials and Manufacturing Processes*, vol. 15, no. 1, pp. 107–122, 2000.

[4] C. Lee, S. Kim, H. Kim, and S.-H. Ahn, "Measurement of anisotropic compressive strength of rapid prototyping parts," *Journal of Materials Processing Technology*, vol. 187-188, pp. 627–630, 2007.

[5] H. G. Harris and G. Sabnis, *Structural modelling and experimental techniques*. CRC Press, second ed., 1999.

[6] "ASTM E1876-15: Standard Test Method for Dynamic Young's Modulus, Shear Modulus, and Poisson's Ratio by Impulse Excitation of Vibration," 2015.

[7] T. G. Carne, D. T. Griffith, and M. E. Cassias, "Support Conditions for Free Boundary-Condition Modal Testing," *IMAC-XXV: A Conference & Exposition on Structural Dynamics*, no. January 2015, 2007.

[8] "ISO 178:2001: Plastics-Determination of flexural properties," 2003.

[9] A. Grammatikopoulos, P. Temarel, and J. Banks, "Experimental hydroelastic responses of an elastic container ship-inspired barge model produced using additive manufacturing," in *8th International Conference on Hydroelasticity in Marine Technology*, (Seoul, Korea), 2018.